Realization of Rational Models for Tower-Footing Grounding Systems

Antonio C. S. Lima, Thiago J. M. A. Parreiras, Rafael Alípio, and Maria Teresa Correia de Barros

***Abstract*—A tower footing grounding system plays an essential role in lightning-related overvoltages. For time-domain analysis, using an Electromagnetic Transient (EMT) program, one typically has to resort to a rational approximation of the harmonic impedance or a frequency-dependent network equivalent (FDNE) for the grounding system. Although one may obtain a rational approximation in several ways, a discussion of the impact of the topology considered for the rational approximation and the effect of the effective length in this realization has not been presented in the literature. Thus, this work focused on these two aspects. First, a comparison of either approach regarding a minimum-order representation. Second, comparing the two possible topologies of the rational approximation order and its relationship with the effective length. The results indicate that an accurate FDNE is slightly more robust if the effective length is respected.**

***Keywords*—Grounding, Circuit Synthesis, Lightning Protection, Electromagnetic Transients.**

I. Introduction

TOWER-footing grounding system plays an important role in assessing ground potential rise (GPR) during transients related to lighting phenomena. Typically, the frequency or time domains can be used for such evaluation. For the former, the Method of Moments (MoM) [1], [2] is employed, considering either an equivalent impedance matrix [3]–[6] or using the Partial Element Equivalent Circuit (PEEC) method [7], [8] as the Hybrid Electromagnetic Model (HEM) [9], or its modified version (mHEM) [10]. For the latter, there are two main possibilities: The finite-difference Time-Domain (FDTD) can be used to directly derive a ground system immittance [11], [12] or one may adapt the grounding impedance calculated using one of the above methods to allow a representation in an Electromagnetic Transient (EMT) program such as ATP, EMTP or PSCAD.

To include a grounding system in an EMT program, one may consider using a frequency-dependent transmission line model [13]–[16], obtain an equivalent circuit [17]–[20] or use a rational approximation of the harmonic impedance of the grounding system. Some algorithms such as, Vector Fitting [21]–[23] or Matrix Pencil Method [24]–[27] can be utilized to obtain this harmonic impedance.

More recently, in the case of a tower footing grounding system, some works [28], [29] have treated the tower footing grounding system as a frequency-dependent network equivalent (FDNE). In this scenario, post-processing passivity enforcement must be carried out to ensure stable time responses [30]–[34]. However, these works do not discuss whether or not this approach leads to a more robust implementation in terms of numerical stability, realization order, and even if a reduced-order realization is feasible.

The topic of order reduction is vast and has received considerable interest in the technical literature; see, for instance, [35]–[37]. Traditional methods relying on balanced truncation [38], [39] have been shown to fail to provide accurate responses in the high-frequency range, demanding a different approach to achieve minimum order.

The paper is organized as follows. Section II briefly describes the formulation of the impedance matrices using mHEM, and the assembly of an equivalent nodal admittance matrix. Section III-A presents the determination of the harmonic impedance and its associated rational modeling. Section III-B shows the evaluation of an FDNE for the tower footing grounding system and the related rational approximation, together with a discussion of the pole number and the associated accuracy. Time responses of the GPR of the counterpoise configuration considering double-peek and fast-front currents are depicted in Section IV. The main conclusions are presented in Section V.

II. Frequency Domain Modeling

Consider, initially, two arbitrarily oriented lossless electrodes i and k with radius a_i, a_k, and length L_i, L_k, respectively, and immerse in a lossy medium, with a propagation constant $\gamma = \sqrt{j\omega\mu\left(\sigma + j\omega\varepsilon\right)}$. It is assumed that $L_i > a$ and $L_k > a$ and both are electrically short, i.e. , $|\gamma L_i| \ll 1$ and $|\gamma L_k| \ll 1$.

A current $\mathbf{I}$ is injected in electrode i, as both L_k and L_i are electrically short, it can then be divided into a transverse current $\mathbf{I}_T$ distributed along the electrode, which is injected in the surrounding medium, and a longitudinal $\mathbf{I}_L$ along the electrode. The electrical field at an arbitrary point at the surface of electrode k is approximately given by (1) and the electric scalar potential then can approximately be written as (2)

A. C. S. Lima and T. J. M. A. Parreiras are with Universidade Federal do Rio de Janeiro, P.O. Box. 68504, 21945-970, Rio de Janeiro, RJ, Brazil, (emails: acsl@coppe.ufrj.br, masseran@coppe.ufrj.br). R. Alípio is with CEFET-MG, Belo Horizonte, MG, Brazil, (email: rafael.alipio@cefetmg.br). M. T. Correia de Barros is with University of Lisbon, Lisbon, Portugal, (email: teresa.correiadebarros@tecnico.ulisboa.pt).

This study was financed in part by the Coordenação de Aperfeiçoamento de Pessoal de Nível Superior - Brasil (CAPES), Finance Code 001. It was also partially supported by INERGE (Instituto Nacional de Energia Elétrica), CNPq (Conselho Nacional de Desenvolvimento Científico e Tecnológico), and FAPERJ (Fundação Carlos Chagas Filho de Amparo à Pesquisa do Estado do Rio de Janeiro).

Paper submitted to the International Conference on Power Systems Transients (IPST2025) in Guadalajara, Mexico, June 8-12, 2025.

$$\mathbf{E} \approx \frac{j\omega\mu}{4\pi}\,\mathbf{I}_L \exp\left(-\gamma\, R\right) \int\limits_{L_k} \frac{1}{r}\,\cos\phi\, d\xi \tag{1}$$

$$\mathbf{V} \approx \frac{\mathbf{I}_T}{4\pi\left(\sigma + j\omega\varepsilon\right)} \frac{\exp\left(-\gamma\, R\right)}{L_k} \int\limits_{L_k} \frac{1}{r}\, d\xi \tag{2}$$

where r is the distance between an arbitrary infinitesimal element at the center of electrode i to an arbitrary point at the surface of electrode k, ϕ is the angle between the vectors associated with L_i and L_k, and R is the distance between the middle point at the center of conductor i to a point at the surface of conductor k.

These approximations allow the following expressions (3) for the transverse and longitudinal mutual impedances

$$\begin{aligned} Z_{T_{ik}} &= \frac{\exp\left(-\gamma\, R\right)}{4\pi\left(\sigma + j\omega\varepsilon\right) L_i L_k}\overline{P}_{ik} \\ Z_{L_{ik}} &= \frac{j\omega\mu\cos\phi\exp\left(-\gamma\, R\right)}{4\pi}\overline{P}_{ik} \end{aligned} \tag{3}$$

where $\overline{P}_{ik}$ is now given by (4). The distances R_1, R_2, R and the finite length conductors are depicted in Fig. 1.

$$\overline{P}_{ik} = \int\limits_{L_k} \ln \frac{R_1 + R_2 + L_i}{R_1 + R_2 - L_i}\, d\xi \tag{4}$$

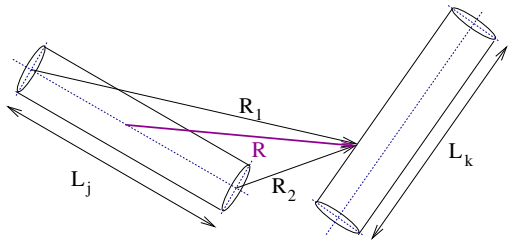

Figure 1. Finite Length lossless electrodes in a uniform medium.

A key aspect is the segmentation of the electrodes. A maximum length of λ/10 was adopted, where λ is the wavelength of the highest frequency of interest for waves propagating in soil. In this research, the maximum frequency of interest is 10 MHz.

To determine the self-elements in these matrices, it is necessary to evaluate both $\mathbf{E}$ and $\mathbf{V}$ at the electrode surface. Conductor losses can easily be included using the well-known expression with Bessel functions. These expressions are well known and can be found in [10], [13].

As elements $\overline{P}_{ik}$ and R are frequency independent, they are calculated only once, considerably reducing the computational burden. To further increase numerical performance, geometrical symmetry is used to reduce the number of necessary evaluations as proposed in [40].

As the distance from the electrodes is sufficiently larger than the electrode radius, a simple charge/current image was considered to avoid a more rigorous solution to represent the air-soil interface via a series expansion of plane waves and then obtain a coherent set of reflection and refraction coefficients [41, sec. 7.6]. Furthermore, in [42], it was shown that image methods can provide suitable response for buried conductors if frequencies below 10 MHz are to be considered.

If one considers $\mathbf{Z}_T$ to be the transverse impedance considering all the segmented conductors and their associated images and $\mathbf{Z}_L$ to be the one related to the longitudinal impedances, the expression (5) can be written

$$\mathbf{Y}_n = \left(\mathbf{m}_A^T \cdot \mathbf{Z}_T^{-1} \cdot \mathbf{m}_A + \mathbf{m}_B^T \cdot \mathbf{Z}_L^{-1} \cdot \mathbf{m}_B\right) \tag{5}$$

where $\mathbf{Y}_n$ is an equivalent nodal admittance matrix for a system of electrodes. The matrices $\mathbf{m}_A$ and $\mathbf{m}_B$ are the incidence matrices obtained through an oriented graph that relates the adjacent nodes and segments.

III. Rational Approximation

A. Tower-footing Grounding System as Harmonic Admittance

In time-domain simulations, the harmonic admittance Y_g is considered instead of the harmonic impedance ($Z_g = Y_g^{-1}$) since a nodal or modified nodal formulation is used. Thus, for the sake of argument, consider a simple counterpoise configuration as depicted in Fig. 2.

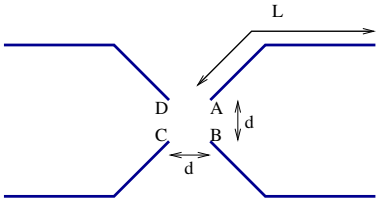

Figure 2. Counterpoise configuration.

To obtain the harmonic impedance Z_g, one must first solve (6) and (7), where $\mathbf{V}$ is the voltage vector for each node to be calculated and $\mathbf{I_n}$ is a vector of injected current.

$$\mathbf{Y}_n \cdot \mathbf{V} = \mathbf{I}_n \tag{6}$$

$$\mathbf{I}_n = [1/4, 0\cdots, 1/4, 0, \cdots, 1/4, 0, \cdots, 1/4, 0, \cdots]^T \tag{7}$$

The values $I_n(i) \neq 0$ corresponds to the injected current at nodes A through D, as shown in Fig. 2.

The ground potential rise (GPR) will be the voltage at node A (V_A). Naturally, in this configuration, $V_A = V_B = V_C = V_D$. Thus, Z_g can be obtained as (8)

$$Z_g = \frac{V_A(\omega)}{1\text{A}} \tag{8}$$

and then the rational approximation is carried out for harmonic admittance by (9), which is rather straightforward, i.e.,

$$Y_g(s) \approx Y_{fit}(s) = R_0 + \sum_{k=1}^{N} \frac{R_k}{s - p_k} \tag{9}$$

where N is the order of the approximation, R_k, and p_k are real or come in pairs of complex conjugates. As mentioned above, the pole relocation algorithm known as vector fitting (VF) is used [22], [43], [44].

As the order N needs to be predefined, one of the goals of this work is to investigate a minimal order realization for a grounding system with suitable accuracy. Initial tests with orders as high as 40 poles indicated that several poles had very small residues, thus contributing little to the frequency response.

In this work, a simple approach was considered to determine the approximation order. An initial estimate of 2 poles and a maximum of 20 poles was considered. This order was chosen based on previous experience with the rational approximation model of frequency-dependent soil parameters [45] indicating that a fitting order near 20 poles should suffice. The heuristic adopted here is based on multiple VF runs, varying the rational approximation order. This order is increased until the rms-error (e_{rms}) obtained through the fitting process reaches a previously defined tolerance, i.e.,

$$\mathrm{e}_{rms} = \sqrt{\frac{\sum_{m=1}^{Ns} |Y_g(s_m) - Y_{fit}(s_m)|^2}{N_s}} \leq \frac{\min(|Y_g(s)|)}{1000} \tag{10}$$

where N_s is the number of frequency samples used. A frequency range from 100 Hz to 10 MHz with 250 logarithmically spaced samples were considered. The stop criterion adopted was similar to the one found in the wide-band modeling of overhead transmission lines and underground cables in EMT programs.

Lastly, a final refinement is carried out based on the idea of the dominant pole [46]–[48]. Thus,

$$\arctan\left(\frac{r_r^i}{p_r^i}\right) \geq \xi \tag{11}$$

where p_r^i is the real part of the i^{th} pole, r_r^i is the real part of the i^{th} residue, and ξ is a pre-defined tolerance. Increasing the value of ξ would lead to lower order model. The set of poles/residues that do not meet this criterion are disregarded. Then, the rational model is refitted using this new reduced set. It was found that with this arrangement a reduction of almost half the number of poles was obtained. Future work will compare this approach with other techniques to obtain a minimal order model.

Table I presents the results for the rational approximation for low-resistivity soils with shorter electrodes and high-resistivity soils with longer electrodes. For the scenarios, relatively low-order realizations were obtained. In all cases, a final model with 11 poles was utilized, and an accurate approximation was obtained with deviations at least three orders of magnitude below the original data.

Table I
FITTING RESULTS CONSIDERING LOW RESISTIVITY AND HIGH RESISTIVITY SOIL WITH DISTINCT ELECTRODE LENGTHS.

length (m)	ρ (Ω·m)	order	$e_{rms} \times 10^{-5}$
30	100	11	3.6925
60	100	11	6.4058
90	1000	11	2.7303
120	1000	11	2.2772

Figure 3 shows the results of the fitting using mHEM, to represent $Y_g(s)$ for the counterpoise in Fig. 2 with $L = 90$ m and for a soil resistivity of $1000\,\Omega \cdot$ m and $\varepsilon_r = 10$.

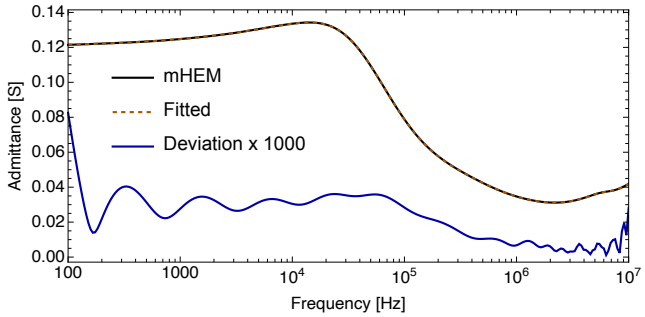

(a) Admittance magnitude

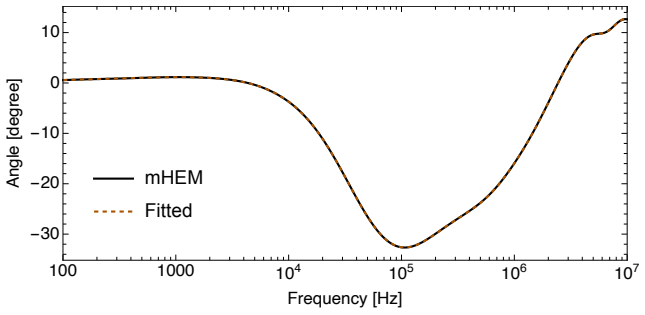

(b) Admittance phase angle

Figure 3. Fitting results considering $L = 90$ m and $\rho = 1000\,\Omega$.m.

The above results may lead one to believe that an order as high as 11 should suffice. However, this is not necessarily true for every grounding system configuration. A considerably higher-order realization is found if the effective length ℓ_{eff} is disregarded [17], [18], [49], i.e., shorter counterpoise in high resistivity soil. The reason for that is twofold. First, the harmonic admittance $Y(\omega)$ presents a higher oscillatory behavior at higher frequencies for higher resistivity soils, see for instance [50]–[53]. Second, if the counterpoise length is shorter than ℓ, higher oscillations are expected as the current along the counterpoise is forced to be null drastically at the end of the counterpoise. This rapid decrease in the current will cause the oscillation at the tail of the harmonic admittance. To illustrate this, consider the results for a 60 m counterpoise in a 1000 Ω·m soil as shown in Fig. 4. This fitting required an order of 28 poles to reach $e_{rms} = 1.1018 \times 10^{-5}$.

B. Tower-footing Grounding System as FDNE

For an FDNE, the procedure is slightly different. Again, consider a simple counterpoise configuration as previously

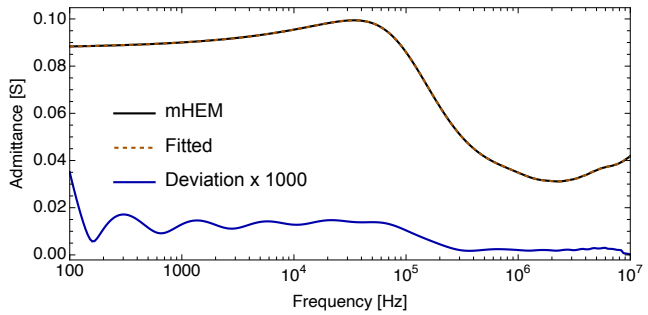

(a) Admittance magnitude

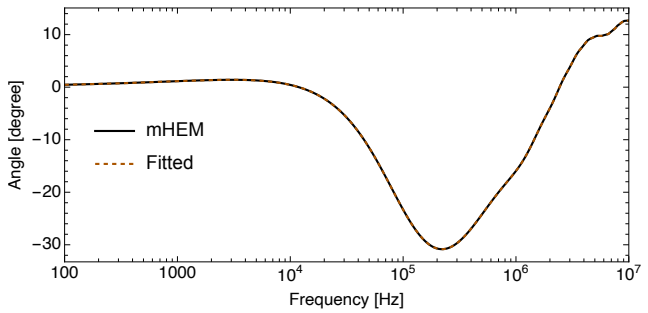

(b) Admittance phase angle

Figure 4. Fitting results considering $L = 60$ m and $\rho = 1000\,\Omega$.m.

evaluated. After calculating $\mathbf{Y}_n$ and obtaining $\mathbf{Z}_n$ ($\mathbf{Z}_n = \mathbf{Y}_n^{-1}$), one extracts the following reduced impedance matrix, which is shown in (12) and can be understood as the driving point impedance of each leg of the counterpoise.

$$\mathbf{Z}_{red} = \begin{bmatrix} Z_{AA} & Z_{AB} & Z_{AC} & Z_{AD} \\ Z_{AB} & Z_{BB} & Z_{BC} & Z_{BD} \\ Z_{AC} & Z_{BC} & Z_{CC} & Z_{CD} \\ Z_{AD} & Z_{BD} & Z_{CD} & Z_{DD} \end{bmatrix} \tag{12}$$

The next step is to obtain the reduced admittance matrix $\mathbf{Y}_{red}$ ($\mathbf{Y}_{red} = \mathbf{Z}_{red}^{-1}$), which will be used as FDNE, through a rational approximation, such as in (13),

$$\mathbf{Y}_{red} \approx \mathbf{Y}_{fit} = \mathbf{G}_0 + \sum_{n=1}^{N} \frac{\mathbf{R}_n}{s + p_n} \tag{13}$$

where $\mathbf{G}_0$ is a conductance matrix related to the low-frequency resistance matrix ($\mathbf{R}_{LF}$ and $\mathbf{G}_0 = \mathbf{R}_{LF}^{-1}$), $\mathbf{R}_n$ are the residues matrices and p_n the poles.

To ensure simulations with stable time-domain responses, it is necessary to assess whether there are passivity violations and enforce the passivity. The former can be evaluated using a Hamiltonian matrix, obtained from the rational approximation, and the latter is achieved through perturbation of the residues matrices as proposed in [30].

The procedure to determine the maximum order was similar to the one used for the scalar model. Only the eigenvalues of $\mathbf{Y}_n(s)$ are used to verify the model accuracy, such as in (14),

$$\mathrm{e}_{rms} \leq \frac{\min(|\lambda_{min}(s)|)}{1000} \tag{14}$$

where $\lambda_{min}(s)$ is the eigenvalue with the smallest amplitude of the admittance matrix $\mathbf{Y}_n(s)$.

Table II presents the results for several scenarios considering shorter electrodes in low-resistivity soil and longer electrodes in high-resistivity soils.

The rational model's fitting order increases when compared with the scalar model. For shorter electrodes, the order increases by around 50%, while longer electrodes presented an increase of over 80%. This is because the mutual elements are not monotonic, presenting some oscillations for frequencies above 10 kHz. The FDNE approach seems more robust since the order is less affected by ℓ_{eff}, as it happens in the scalar case (treating the tower-footing grounding system as a harmonic admittance). Figure 5 depicts the fitting results for the self and mutual admittances considering the shortest and longest electrodes in Table II. The self elements presented higher magnitude throughout the whole frequency range. It can be noticed that even for $L = 30$ and $\rho = 100\,\Omega$·m that some amplitudes oscillations can be found for frequencies around 100 kHz.

This behavior is even more noticeable for the longest counterpoises, where these oscillations appear for frequencies above 50 kHz. The Hamiltonian matrix test indicated no passivity violations, as it can be observed in Fig. 6, which depicts the behavior of the real part of the eigenvalues (λ) of the admittance matrix ($\mathbf{Y}_{fit}$), i.e., $\lambda = \mathrm{eig}\,(\mathbf{Y}_{fit})$.

Table II
FITTING RESULTS CONSIDERING LOW RESISTIVITY AND HIGH RESISTIVITY SOIL WITH DISTINCT ELECTRODE LENGTHS FOR COUNTERPOISE TREATED AS FDNE.

length (m)	ρ (Ω·m)	order	$e_{rms} \times 10^{-6}$
30	100	16	1.0197
60	100	17	1.3129
90	1000	22	0.6179
120	1000	20	0.7739

C. Realization Using a Unique Order

From an implementation point of view, it would be interesting to have a unique order regardless of the tower footing grounding system considered and its realization. Thus, it is investigated whether the highest order, $N = 22$, found in FDNE rational approximation, would also provide suitable responses in the other scenarios considered in this work.

The results of the analysis above are presented in Table III, where it can be observed that, For short counterpoise in low resistivity soils, the scalar approach (fitting the harmonic admittance) seems to provide an improved response compared to the FDNE approach. The FDNE formulation provided slightly more accurate responses for longer counterpoises in high-resistivity soils and presented no numerical issues as passivity violations.

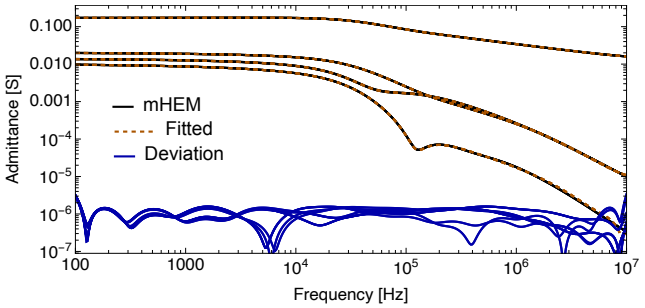

(a) Admittance Magnitude for $L = 30$ m and $\rho = 100\,\Omega$.m

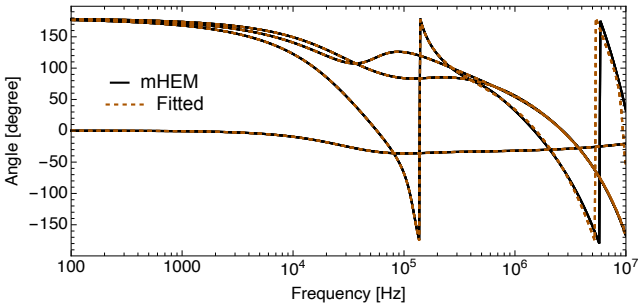

(b) Admittance phase angles for $L = 30$ m and $\rho = 100\,\Omega$.m

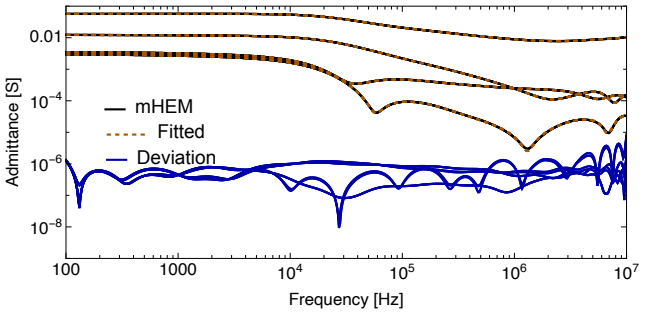

(c) Admittance Magnitude for $L = 120$ m and $\rho = 1000\,\Omega$.m

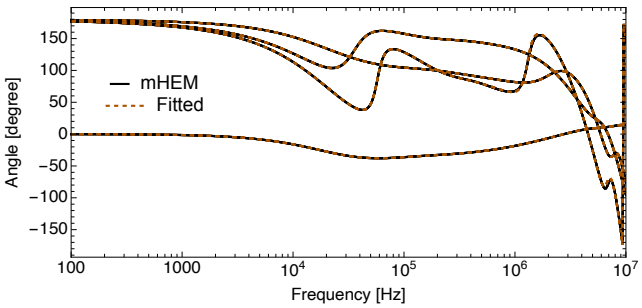

(d) Admittance phase angle for $L = 120$ m and $\rho = 1000\,\Omega$.m

Figure 5. Fitting results considering distinct counterpoise lengths and soil resistivities.

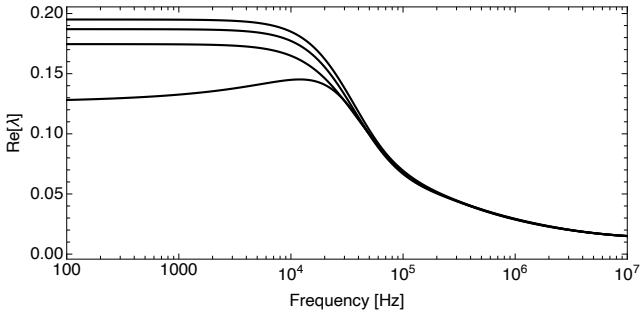

(a) $L = 30$ m and $\rho = 100\,\Omega$.m

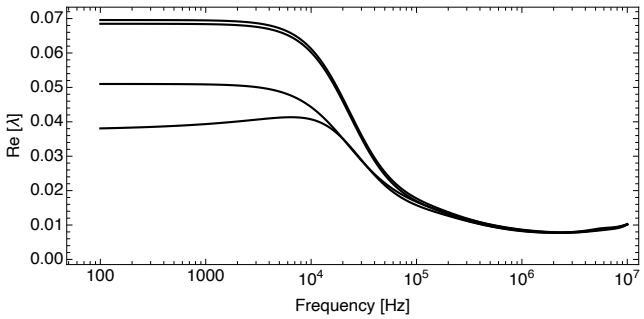

(b) $L = 120$ m and $\rho = 1000\,\Omega$.m

Figure 6. Real part of the eigenvalues of fitted FDNE.

IV. Time Responses

For the evaluation of the time responses, two "types" of the injected currents are considered, both are based on return current strokes measured at Mount San Salvatore. One of these currents has a double peak and is related to the first negative stroke, while the second has a fast front commonly associated with subsequent strokes. Fig. 7 represents these two injected current waveforms.

Table III
Fitting results considering 22 poles for all topologies.

length (m)	ρ (Ω·m)	$e_{rms} \times 10^{-6}$	topology
30	100	0.0543	FDNE
30	100	0.0281	scalar
60	100	0.0901	FDNE
60	100	0.0281	scalar
90	100	0.1292	FDNE
90	100	0.0615	scalar
120	100	0.2135	FDNE
120	100	0.04471	scalar
30	1000	1.4360	FDNE
30	1000	1.0482	scalar
60	1000	5.2965	FDNE
60	1000	3.4647	scalar
90	1000	0.6179	FDNE
90	1000	2.3829	scalar
120	1000	0.347	FDNE
120	1000	1.2551	scalar

For the analytical representation of this current, it is considered a series of Heidler functions, such as (15) proposed in [54],

$$i(t) = \sum_{k=1}^{K} \frac{I_{0_k}}{\eta_k} \left[\frac{(t/\tau_{1k})^{n_k}}{1 + (t/\tau_{1k})^{n_k}} \right] \exp\left(-\frac{t}{\tau_{2k}} \right)$$
$$\eta_k = \exp\left(-\frac{\tau_{1k}}{\tau_{2k}} \cdot \left(\frac{n_k\, t_{2k}}{\tau_{1k}} \right)^{1/n_k} \right) \tag{15}$$

where K, I_{0_k}, τ_{1k}, τ_{2k}, n_k and η_k are adjustable parameters of the injected current waveforms.

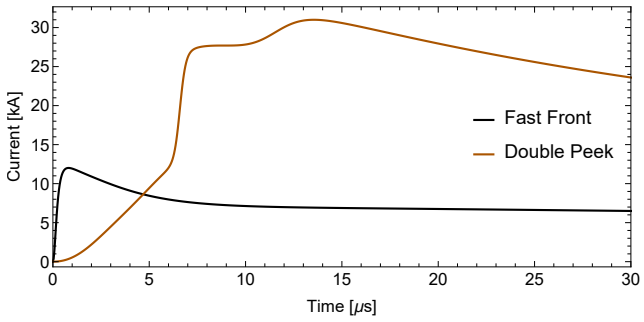

Figure 7. Waveform of injected current considered for the transient analysis of a tower-footing grounding system.

For the frequency domain analysis using the NLT, 1024 samples, with a maximum observation time of 40 μs, is considered, leading to a time-step of 39.062 ns. A stand-alone program written in the Wolfram Language in an environment similar to the matEMTP [55] is used for the time-domain analysis. In this case, a time-step of 5 ns with a maximum time of 40μs is considered. This leads to 8000 samples for the time-domain simulation. The time-step in the EMT-type of the simulation was chosen to lead a Nyquist frequency of 10 MHz which was the largest frequency of interest in the rational approximation.

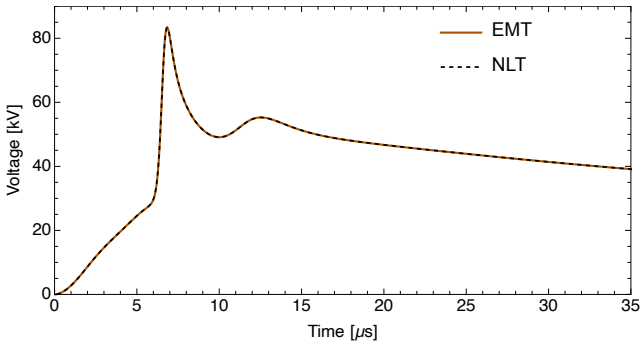

(a) $L = 30$ m and $\rho = 100\,\Omega$.m

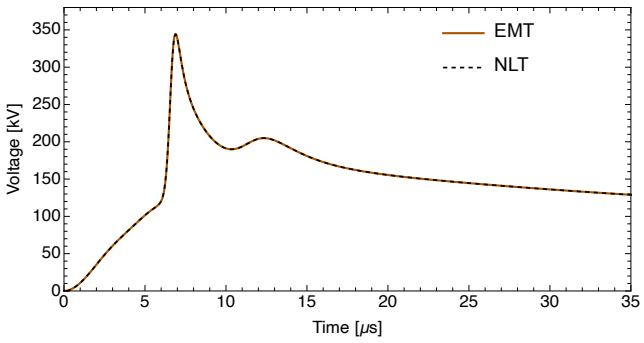

(b) $L = 120$ m and $\rho = 1000\,\Omega$.m

Figure 8. Ground potential rise considering the double peek current.

The counterpoise considered is the one found in Fig. 2 with $L = 30$ m and $\rho = 100\,\Omega$·m and with $L = 120$ m and $\rho = 1000\,\Omega$·m. The results are presented in Fig. 8 for the double peak current and in Fig. 9 for the fast current wave. The GPR calculated through both methodologies is shown to be almost coincident, regardless of the current excitation. The

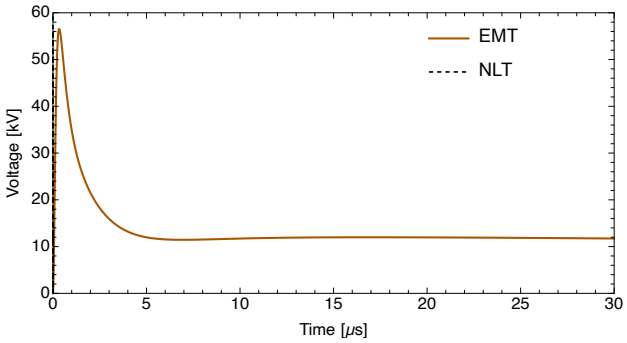

(a) $L = 30$ m and $\rho = 100\,\Omega$.m

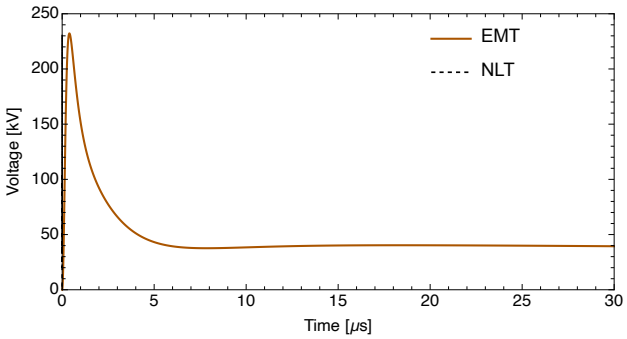

(b) $L = 120$ m and $\rho = 1000\,\Omega$.m

Figure 9. Ground potential rise for fast front current.

results obtained using the scalar formulation were identical to those of the FDNE.

A computation burden assessment was made, where it was considered the time to evaluate the 250 samples, obtain the reduced matrix in the FDNE case or the harmonic admittance, the rational approximation evaluation, the passivity verification for the FDNE case and the time spent in the time-step loop to obtain the time responses.

The total computation time was around 25% faster for harmonic admittance and around 45% for FDNE, when comparing these approaches with the NLT. All these timings were obtained considering an i9 Intel personal computer with 16GB of RAM.

V. Conclusions

This work compares two approaches for a rational approximation of a tower footing grounding system aiming for a time-domain analysis using an EMT program. It shows that, despite the more straightforward approach, the scalar model representation of the tower footing ground system can only be used with a lower order if the effective length is respected. Suppose a more detailed representation is considered, such as treating the tower footing grounding system as an FDNE based on the driving point impedance of each counterpoise leg. In that case, a higher order is needed for the realization. However, lower-order variations were found. The last approach seems more robust for this kind of analysis. With a rational realization with 22 poles, the harmonic admittance and FDNE can be fitted with acceptable accuracy, regardless of the counterpoise length and soil resistivity.

Future work will deal with the analysis of other criteria for the pole reduction as well as the assessment of the transient propagation of the electromagnetic field on the ground due to lightning-related currents, as it will demand only an increase in the order utilized in the FDNE approach, considering key points along the counterpoise. Probably, it should consider an adaptive segmentation scheme, where a coarse segmentation could be used for conductors away from the region of interest and a fine segmentation could be used for the ones close to the region of interest.

REFERENCES

[1] R. F. Harrington, *Field Computation by Moment Method*, D. G. D. U. of Arizona, Ed. IEEE PRESS Series on Electromagnetic Waves, 1993.

[2] ——, *Time-Harmonic Electromagnetic Fields*, ser. The IEEE Press Series on Electromagnetic Wave Theory. Piscatawat, NJ: IEEE Press, 2001, reissue of 1961 edition.

[3] L. Grcev and F. Dawalibi, "An electromagnetic model for transients in grounding systems," *IEEE Trans. on Power Delivery*, vol. 5, no. 4, pp. 1773 –1781, oct 1990.

[4] L. D. Grcev, "Computer analysis of transient voltages in large grounding systems," *IEEE Transactions on power delivery*, vol. 11, no. 2, pp. 815–823, 1996.

[5] L. D. Grcev and M. Heimbach, "Frequency dependent and transient characteristics of substation grounding systems," *IEEE Transactions on Power Delivery*, vol. 12, no. 1, pp. 172–178, Jan 1997.

[6] M. Heimbach and L. Grcev, "Grounding system analysis in transients programs applying electromagnetic field approach," *IEEE Trans. on Power Delivery*, vol. 12, no. 1, pp. 186 –193, jan 1997.

[7] A. Ruehli, "Partial element equivalent circuit (PEEC) method and its application in the frequency and time domain," in *Electromagnetic Compatibility, 1996. Symposium Record. IEEE 1996 International Symposium on*. IEEE, 1996, pp. 128–133.

[8] P. Yutthagowith, A. Ametani, N. Nagaoka, and Y. Baba, "Application of the partial element equivalent circuit method to analysis of transient potential rises in grounding systems," *IEEE Transactions on Electromagnetic Compatibility*, vol. 53, no. 3, pp. 726–736, 2011.

[9] S. Visacro and A. Soares, "HEM: A model for simulation of lightning-related engineering problems," *IEEE Trans. on Power Delivery*, vol. 20, no. 2, pp. 1206–1208, 2005.

[10] A. C. S. Lima, R. A. R. Moura, P. H. N. Vieira, M. A. O. Schroeder, and M. T. Correia de Barros, "A computational improvement in grounding systems transient analysis," *IEEE Transactions on Electromagnetic Compatibility*, vol. 62, no. 3, pp. 765–773, 2020.

[11] Y. Baba, N. Nagaoka, and A. Ametani, "Modeling of thin wires in a lossy medium for fdtd simulations," *IEEE Transactions on Electromagnetic Compatibility*, vol. 47, no. 1, pp. 54–60, 2005.

[12] M. Tsumura, Y. Baba, N. Nagaoka, and A. Ametani, "FDTD simulation of a horizontal grounding electrode and modeling of its equivalent circuit," *IEEE transactions on electromagnetic compatibility*, vol. 48, no. 4, pp. 817–825, 2006.

[13] E. D. Sunde, *Earth conduction effects in transmission systems*. Dover Publications Inc., 1949.

[14] F. Menter and L. Grcev, "Emtp-based model for grounding system analysis," *IEEE Trans. on Power Delivery*, vol. 9, no. 4, pp. 1838 –1849, oct 1994.

[15] Y. Liu, M. Zitnik, and R. Thottappillil, "An improved transmission-line model of grounding system," *IEEE Transactions on Electromagnetic Compatibility*, vol. 43, no. 3, pp. 348–355, 2001.

[16] Y. Liu, N. Theethayi, and R. Thottappillil, "An engineering model for transient analysis of grounding system under lightning strikes: nonuniform transmission-line approach," *IEEE Transactions on Power Delivery*, vol. 20, no. 2, pp. 722–730, April 2005.

[17] L. Grcev, "Impulse efficiency of ground electrodes," *IEEE Transactions on Power Delivery*, vol. 24, no. 1, pp. 441–451, Jan 2009.

[18] ——, "Modeling of grounding electrodes under lightning currents," *IEEE Transactions on Electromagnetic Compatibility*, vol. 51, no. 3, pp. 559–571, 2009.

[19] L. D. Grcev, A. Kuhar, V. Arnautovski-Toseva, and B. Markovski, "Evaluation of High-Frequency circuit models for horizontal and vertical grounding electrodes," *IEEE Transactions on Power Delivery*, vol. 33, no. 6, pp. 3065–3074, Dec 2018.

[20] L. Grcev, B. Markovski, and M. Todorovski, "General formulas for lightning impulse impedance of horizontal and vertical grounding electrodes," *IEEE Transactions on Power Delivery*, vol. 36, no. 4, pp. 2245–2248, 2021.

[21] B. Gustavsen and A. Semlyen, "Rational approximation of frequency domain responses by vector fitting," *IEEE Trans. on Power Delivery*, vol. 14, no. 3, pp. 1052–1061, Jul. 1999.

[22] B. Gustavsen, "Improving the pole relocating properties of vector fitting," *IEEE Trans. on Power Delivery*, vol. 21, no. 3, pp. 1587–1592, Jul. 2006.

[23] D. Deschrijver, M. Mrozowski, T. Dhaene, and D. De Zutter, "Macromodeling of multiport systems using a fast implementation of the vector fitting method," *IEEE Microwave and Wireless Components Letters*, vol. 18, no. 6, pp. 383–385, Jun. 2008.

[24] T. K. Sarkar and O. Pereira, "Using the matrix pencil method to estimate the parameters of a sum of complex exponentials," *IEEE Antennas and Propagation Magazine*, vol. 37, no. 1, pp. 48–55, 1995.

[25] K. Sheshyekani, H. R. Karami, P. Dehkhoda, M. Paolone, and F. Rachidi, "Application of the matrix pencil method to rational fitting of frequency-domain responses," *IEEE Trans. on Power Delivery*, vol. 27, no. 4, pp. 2399–2408, 2012.

[26] K. Sheshyekani, M. Akbari, B. Tabei, and R. Kazemi, "Wideband modeling of large grounding systems to interface with electromagnetic transient solvers," *IEEE Transactions on Power Delivery*, vol. 29, no. 4, pp. 1868–1876, 2014.

[27] J. Morales Rodriguez, E. Medina, J. Mahseredjian, A. Ramirez, K. Sheshyekani, and I. Kocar, "Frequency-domain fitting techniques: A review," *IEEE Transactions on Power Delivery*, vol. 35, no. 3, pp. 1102–1110, 2020.

[28] M. R. Alemi and K. Sheshyekani, "Wide-band modeling of tower-footing grounding systems for the evaluation of lightning performance of transmission lines," *IEEE Transactions on Electromagnetic Compatibility*, vol. 57, no. 6, pp. 1627–1636, 2015.

[29] R. Shariatinasab, J. Gholinezhad, K. Sheshyekani, and M. R. Alemi, "The effect of wide band modeling of tower-footing grounding system on the lightning performance of transmission lines: A probabilistic evaluation," *Electric Power Systems Research*, vol. 141, pp. 1–10, 2016. [Online]. Available: https://www.sciencedirect.com/science/article/pii/S0378779616302486

[30] B. Gustavsen, "Fast passivity enforcement for pole-residue models by perturbation of residue matrix eigenvalues," *IEEE Trans. on Power Delivery*, vol. 23, no. 4, pp. 2278 –2285, oct. 2008.

[31] A. Semlyen and B. Gustavsen, "A half-size singularity test matrix for fast and reliable passivity assessment of rational models," *IEEE Trans. Power Delivery*, vol. 24, no. 1, pp. 345–351, Jan. 2009.

[32] J. Morales, J. Mahseredjian, K. Sheshyekani, A. Ramirez, E. Medina, and I. Kocar, "Pole-selective residue perturbation technique for passivity enforcement of fdnes," *IEEE Transactions on Power Delivery*, vol. 33, no. 6, pp. 2746–2754, 2018.

[33] E. Medina, A. Ramirez, J. Morales, and J. Mahseredjian, "Alternative approach to alleviate passivity violations of rational-based fitted functions," *IEEE Transactions on Power Delivery*, vol. 34, no. 3, pp. 1161–1170, 2019.

[34] J. Becerra, I. Kocar, K. Sheshyekani, and J. Mahseredjian, "Passivity enforcement of wideband line model through coupled perturbation of residues and poles," *Electric Power Systems Research*, vol. 190, p. 106798, 2021. [Online]. Available: https://www.sciencedirect.com/science/article/pii/S0378779620306015

[35] P. Benner, W. Schilders, S. Grivet-Talocia, A. Quarteroni, G. Rozza, and L. Miguel Silveira, Eds., *Model Order Reduction: Volume 3 applications*. De Gruyter, 2020.

[36] P. Benner, W. Schilders, S. Grivet-Talocia, A. Quarteroni, G. Rozza, and L. Miguel Silveira, *Model Order Reduction: Volume 2: Snapshot-Based Methods and Algorithms*. De Gruyter, 2020.

[37] P. B. Stefano Grivet-Talocia Alfio Quarteroni Gianluigi Rozza Wil Schilders Luís Miguel Silveira, Ed., *Model Order Reduction: Volume 1 System- and Data-Driven Methods and Algorithms*. De Gruyter, 2021. [Online]. Available: https://doi.org/10.1515/9783110498967

[38] M. Safonov and R. Chiang, "A schur method for balanced-truncation model reduction," *IEEE Transactions on Automatic Control*, vol. 34, no. 7, pp. 729–733, 1989.

[39] G. Wang, V. Sreeram, and W. Liu, "A new frequency-weighted balanced truncation method and an error bound," *IEEE Transactions on Automatic Control*, vol. 44, no. 9, pp. 1734–1737, 1999.

[40] P. H. Vieira, R. A. Moura, M. A. O. Schroeder, and A. C. Lima, "Symmetry exploitation to reduce impedance evaluations in grounding grids," *International Journal of Electrical Power & Energy Systems*, vol. 123, p. 106268, 2020. [Online]. Available: https://www.sciencedirect.com/science/article/pii/S0142061519342188

[41] J. A. Stratton, *Electromagnetic Theory*. McGraw-Hill Co., 1941.

[42] V. Arnautovski-Toseva and L. Grcev, "On the image model of a buried horizontal wire," *IEEE Transactions on Electromagnetic Compatibility*, vol. 58, no. 1, pp. 278–286, Feb 2016.

[43] B. Gustavsen and A. Semlyen, "Rational approximation of frequency domain responses by vector fitting," *IEEE Trans. on Power Delivery*, vol. 14, no. 3, pp. 1052–1061, Jul. 1999.

[44] D. Deschrijver, B. Gustavsen, and T. Dhaene, "Advancements in iterative methods for rational approximation in the frequency domain," *IEEE Trans. on Power Delivery*, vol. 22, no. 3, pp. 1633–1642, Jul. 2007.

[45] J. P. L. Salvador, R. Alipio, A. C. S. Lima, and M. T. Correia de Barros, "A concise approach of soil models for time-domain analysis," *IEEE Transactions on Electromagnetic Compatibility*, vol. 62, no. 5, pp. 1772–1779, 2020.

[46] S. Gomes, N. Martins, and C. Portela, "Computing small-signal stability boundaries for large-scale power systems," *IEEE Transactions on Power Systems*, vol. 18, no. 2, pp. 747–752, 2003.

[47] N. Martins, C. Portela, and S. Gomes, "Sequential computation of transfer function dominant poles of s-domain system models," *IEEE Transactions on Power Systems*, vol. 24, no. 2, pp. 776–784, 2009.

[48] S. Gomes Jr, C. Guimarães, N. Martins, and G. Taranto, "Damped nyquist plot for a pole placement design of power system stabilizers," *Electric Power Systems Research*, vol. 158, pp. 158–169, 2018.

[49] J. He, Y. Gao, R. Zeng, J. Zou, X. Liang, B. Zhang, J. Lee, and S. Chang, "Effective length of counterpoise wire under lightning current," *IEEE Transactions on Power Delivery*, vol. 20, no. 2, pp. 1585–1591, 2005.

[50] W. L. M. de Azevedo, A. R. J. de Araújo, J. S. L. Colqui, J. L. A. D'Annibale, and J. P. Filho, "Alternative study to reduce backflashovers using tower-footing grounding systems with multiple inclined rods," *Electric Power Systems Research*, vol. 214, p. 108893, 2023. [Online]. Available: https://www.sciencedirect.com/science/article/pii/S0378779622009440

[51] M. Ghomi, F. Faria da Silva, A. A. Shayegani Akmal, and C. Leth Bak, "Transient overvoltage analysis in the medium voltage substations based on full-wave modeling of two-layer grounding system," *Electric Power Systems Research*, vol. 211, p. 108139, 2022. [Online]. Available: https://www.sciencedirect.com/science/article/pii/S0378779622003613

[52] J. Colqui, A. de Araújo, C. M. de Seixas, S. Kurokawa, and J. Pissolato Filho, "Performance of the recursive methods applied to compute the transient responses on grounding systems," *Electric Power Systems Research*, vol. 196, p. 107281, 2021. [Online]. Available: https://www.sciencedirect.com/science/article/pii/S0378779621002625

[53] E. Stracqualursi, R. Araneo, A. Andreotti, J. B. Faria, F. H. Silveira, and S. Visacro, "Effects of macromodeling on the simulation of transient events caused by direct lightning to overhead power lines," *Electric Power Systems Research*, vol. 235, p. 110866, 2024. [Online]. Available: https://www.sciencedirect.com/science/article/pii/S0378779624007521

[54] A. De Conti and S. Visacro, "Analytical representation of single and double-peaked lightning current waveforms," *IEEE Trans. on Electromagnetic Compatibility*, vol. 49, no. 2, pp. 448–451, May 2007.

[55] J. Mahseredjian and F. Alvarado, "Creating an electromagnetic transients program in matlab: Matemtp," *IEEE Transactions on Power Delivery*, vol. 12, no. 1, pp. 380–388, 1997.